

Torsional warping eigenmodes of FGM beams with longitudinally varying material properties

Justin Murin¹, Mehdi Aminbaghai², Juraj Hrabovsky¹, Giuseppe Balduzzi²,
Michael Dorn³, Herbert A. Mang^{2,4}

¹Department of Applied Mechanics and Mechatronics, IAMM FEI STU,
Bratislava, Ilkovičova 3, 812 19 Bratislava, Slovakia
justin.murin@stuba.sk, juraj.hrabovsky@stuba.sk

²Vienna University of Technology, Institute for Mechanics of Materials and
Structures, Karlsplatz 13, A-1040 Vienna, Austria
mehdi.aminbaghai@tuwien.ac.at, giuseppe.balduzzi@tuwien.ac.at,
herbert.mang@tuwien.ac.at

³Department of Building Technology, Linnaeus University,
Pelarplatsen 1, 351 95 Växjö, Sweden
michael.dorn@lnu.se

⁴National RPGE Chair Professor, Tongji University, Siping Road 1239, Shanghai,
China, herbert.mang@tuwien.ac.at

This document is the accepted version of a work that was published in Engineering Structures. To access the final edited and published work see, <https://doi.org/10.1016/j.engstruct.2018.08.048>. This manuscript version is made available under the CC-BY-NC-ND 4.0 license <https://creativecommons.org/licenses/by-nc-nd/4.0/>.

Keywords: Functionally graded material beams, Longitudinally varying material properties, Non-uniform torsion, Warping torsional eigenvibrations, Deformation due to the secondary torsion moment

Abstract

In this paper, the influence of torsional warping of thin-walled cross-sections of twisted Functionally Graded Material (FGM) beams with a longitudinal polynomial variation of the material properties on their eigenvibrations is investigated, considering the secondary deformations due to the angle of twist. The transfer relations needed for the transfer matrix method are derived. Based on them, the local finite element equations of the twisted FGM beam are established. The warping part of the first derivative of the twist angle, caused by the bimoment, is considered as an additional degree of freedom at the beam nodes. The focus of the numerical

investigation, with and without consideration of the Deformation due to the Secondary Torsional Moment (STMDE), is on modal analysis of straight cantilever FGM beams with doubly symmetric open and closed cross-sections. The influence of the longitudinal variation of the material properties and the secondary torsion moment on the eigenfrequencies is investigated. The obtained results are compared with the ones calculated by a very fine mesh of standard solid and warping beam finite elements.

1.Introduction

The effect of non-uniform torsion on the results of elastostatic and elastodynamic structural analysis of thin-walled beams with both open and closed cross-sections may be significant. The maximum normal stress due to the bimoment occurs at the points of action of external torques (except for free ends of beams) and at cross-sections of restrained warping (e.g. clamped cross-sections). A comprehensive overview of the literature, dealing with the issue of non-uniform torsion can be found, e.g., in [1, 2]. Latest research results have shown that for non-uniform torsion of beams with closed cross-sections the impact of the Secondary Torsion Moment Deformation Effect (STMDE) is particularly significant.

Beam structures are often exposed to time-dependent loads. Commercial FEM codes allow performing modal and transient dynamic analysis by 3D finite beam elements with and without consideration of the warping effect [3-5]. For torsion, very often an improved Saint-Venant theory is used and special mass matrices are proposed. In general, the bicurvature is chosen as an additional warping degree of freedom, and the STMDE is not considered. The beam element in [4] can be used with a lumped or a consistent mass matrix. In the consistent mass matrix the warping effect is considered, but the effect of shear deformations is disregarded. For standard beam elements, the consistent mass matrix is based on [6], with the exception of additional terms arising from the warping constant I_{ω} . For the warping element, lumped masses for the warping degree of freedom (bicurvature) are defined [7]. As stated in [4], for solid and closed thin-walled sections, standard finite beam elements can be used without significant error. However, for open thin-walled sections, warping finite beam elements should be used [5]. In [8], a boundary element method is described for the non-uniform torsional vibration problem of doubly symmetric constant cross-sections, taking non-uniform warping and the STMDE into account. Dynamic analysis of 3D beam elements, restrained at their edges, subjected to arbitrarily distributed dynamic loading, is the topic of [9]. In [10], Ref. [8] is extended by taking geometrical nonlinearity into account, and in [11], the effect of rotary and warping inertia is considered. Nonlinear torsional vibrations of thin-walled beams, exhibiting primary and secondary warping, are investigated in [12]. A solution for the vibration of Timoshenko beams by the isogeometric approach is presented in [13]. The warping effect, however, is not considered. In [14], geometrically non-linear free and forced vibrations of beams with non-symmetrical cross-sections are investigated by the Saint-Venant theory of torsion. Axial-torsional vibrations of rotating pretwisted thin-walled composite box beams, exhibiting primary and secondary warping, are investigated in [15]. The formulation of a 3D beam element for transversal and

warping eigenmode analysis is calculated in [16]. In [17], a new 3D beam finite element for geometrically nonlinear analysis of FGM structures with transversely varying material properties is presented. An accurate prediction of the warping displacements has been achieved.

In [1], the influence of torsional warping of open and closed cross-sections of twisted beams with constant material properties on their eigenvibrations is investigated, considering the secondary deformations due to the angle of twist. Since the bicurvature cannot be used in the constraint equations, see. e.g.[4], the part of the first derivative of the angle of twist, caused by the bimoment as the warping degree of freedom [18], was also used for modal analysis. The result from modal analysis concerning non-uniform and uniform torsion of beams with open cross-sections has shown large differences of the eigenfrequencies. This has proved the well-known fact that the warping effect must be taken into account also for modal analysis of beams with open cross-sections subjected to torsion. It was also shown that the STMDE does not play a significant role in torsion of beams with open cross-sections. In contrast to such cross-sections, the influence of warping (with or without STMDE) on the non-uniform torsional eigenfrequencies of beams with rectangular hollow cross-sections is not significant. The best agreement of the results obtained by solid finite elements and the method proposed in [1] (as well as by the Saint-Venant and the warping beam solutions) is achieved for the 1st torsional eigenfrequency. For the higher modes the differences between corresponding results are increasing. The higher torsional eigenmodes, calculated by solid finite elements, have shown significant deformations of the beam walls (known as the distortion of the cross-section), especially for short beams. This effect cannot be considered by finite beam elements with restrained and unrestrained warping, without additional restrictions. As shown in [19], all eigenfrequencies, calculated by solid finite elements, agree very well with results obtained by experimental measurements. Finally, in [2], a boundary element solution for non-uniform warping dynamic analysis of beams with arbitrary cross-sections, including consideration of shear lag effects due to both flexure and torsion, is described. High accuracy, compared to the solid finite element solution was obtained, but in the solid model the distortion effect of the cross-section was restricted. In [24], the distortional effect of the cross-sections is considered by means of additional degrees of freedom, included in elastostatic analysis of curved beams. A common feature of the cited articles is that constant material properties of the beams in the longitudinal direction are assumed.

Novel engineering technologies face the challenge of answering increasingly complex questions about the functionality of the developed systems. In material science, one of the ground-breaking technologies are functionally graded materials (FGMs), where the material properties are spatially graded. Natural biomaterials often possess the structure of FGMs, which allow them to satisfy requirements such as corrosion resistance, thermal conductivity, strength, elastic stability, fatigue durability, dynamic stability, etc. Fabrication of such materials is complicated, but progress in this area has been significant in recent years. FGMs are obtained the same as a mixture of two or more constituents of almost the same geometry and dimensions. Plasma spraying, powder metallurgy, 3D printing and other technologies are used for fabrication of such

materials. From the macroscopic point of view, FGMs are isotropic at each material point, but the material properties can vary continuously or discontinuously in one, two, or three directions. The variation of the macroscopic material properties can be caused by varying the volume fraction of the constituents or their material. Important structural components made of FGMs are beams. Thin-walled beams play an important role not only in structural applications, but also in thermal, thermo-electric-structural or electric-thermal-structural systems (e.g. MEMS actuators), and in mechatronics. In all of thermo-electric-structural applications, new materials, such as FGMs, can greatly improve the efficiency of engineering systems.

In this paper, [1] is extended to uniform and non-uniform modal analysis of FGM beams with continuously varying material properties in the longitudinal direction. The longitudinal variability of the material properties covers a wide range of possible practical applications. Moreover, it facilitates the establishment and the treatment of the mathematical model of such composite beams. In Chapter 2, a brief summary of the differential equations for Saint-Venant and non-uniform torsional deformations including inertial line moments is formulated. In non-uniform torsion, the part of the bicurvature caused by the bimoment is taken into account as the warping degree of freedom, and the STMDE is also considered. A general semi-analytical solution of the differential equation is presented, and the transfer matrix relation is established, from which the finite element equations of straight warping torsion (WT) finite beam elements with two-nodes are derived. Omitting the external load, the FEM equation for torsional natural free vibrations is obtained.

Chapter 3 contains the numerical investigation. The results from modal analysis of cantilever beams with open I cross-sections and rectangular hollow cross-sections are presented and compared with results obtained from commercial FEM codes. The effect of the longitudinally varying material properties is evaluated. A final assessment of the proposed method is contained in the conclusions.

The main novelty of this paper is the inclusion of the longitudinal variation of the material properties in the differential equations for uniform and non-uniform torsion-free vibrations. The transfer relations are derived, from which equations for the finite beam element for calculation of the torsional eigenfrequencies of straight beams including warping are deduced. The bimoment and the primary part of the bicurvature are also used for specification of the boundary conditions. The proposed approach is applied to non-uniform torsional modal analysis of beams with open and closed cross-sections.

2. Torsional eigenvibrations of FGM beams with longitudinally varying material properties

In the following, the differential equations with variable parameters for torsional eigenvibrations of FGM beams with doubly symmetric open or closed cross-sections are presented. A polynomial variation of the material properties in the longitudinal direction of the beams is considered. The solution of the differential equations is based

on the concept of transfer functions. After derivation of the transfer matrix, the local finite element equation for uniform and non-uniform torsion is established.

2.1 Eigenvibrations of FGM beams due to uniform (Saint-Venant) torsion

Fig. 1 refers to determination of the torsional eigenvibrations (Saint-Venant torsion). It contains the definition of a positive torsional moment $M_T(x)$ and of the corresponding twist angle $\psi(x)$ at the nodes i and j of a straight beam according to the Transfer Matrix Method (TMM) and the Finite Element Method (FEM).

The structures, investigated in this paper, are single beams. As regards the FEM, they can be analyzed by just one single finite element. The results are compared to the ones obtained by the TMM which, contrary to the FEM, does not allow the analysis of frames. Lack of the possibility of comparing the results from FE analysis of frames with results from another method of analysis of such structures the reason for restricting this work to the analysis of single beams.

The beams are loaded by the inertial torsional line moment $\omega^2 I_p \rho(x) \psi(x)$, where I_p denotes the polar moment of area, $\rho(x)$ is the effective longitudinally varying mass density for torsion, and ω is the circular frequency. This inertial line moment represents the static equivalent of the dynamic action. The coordinate $x \in \langle 0, L \rangle$, where L is the length of the beams; $m_T(x)$ is the torsional line moment, which is equal to zero for modal analysis. Constant doubly symmetric, open as well as closed cross-sections are considered. The differential equations of uniform torsion of a beam are formulated in the framework of the TMM. They are given as follows:

$$M_T'(x) = -m_T(x) - \omega^2 I_p \rho(x) \psi(x), \quad (1)$$

$$\psi'(x) = \frac{M_T(x)}{G(x)I_T}. \quad (2)$$

In (4), \bar{b}_{kT} and \bar{b}'_{kT} , ($k \in \langle 0, p_{mT} + 2 \rangle$), are the transfer functions for torsion and their first derivatives, respectively, They represent the solution functions of the differential equation (3). The transfer functions depend on the longitudinal variation of the torsional shear modulus, the natural frequency, the polar moment of inertia, the torsion constant, and the consistent mass density distribution. By inserting (1) and (2) into (4), the transfer matrix relations for the particular case of uniform torsional free vibrations are obtained, after some mathematical manipulations, as follows:

$$\begin{aligned} \begin{bmatrix} \psi(x) \\ M_T(x) \end{bmatrix} &= \begin{bmatrix} A_{1,1}(x) = \bar{b}_{0T}(x) & A_{1,2}(x) = \frac{\bar{b}_{1T}(x)}{I_T G(x)|_{x=0}} \\ A_{2,1}(x) = I_T G(x) \bar{b}'_{0T}(x) & A_{2,2}(x) = \frac{I_T G(x)}{I_T G(x)|_{x=0}} \bar{b}'_{1T}(x) \end{bmatrix} \cdot \begin{bmatrix} \psi_i \\ M_{T,i} \end{bmatrix} \\ &+ \begin{bmatrix} A_{1,3}(x) = -\sum_{k=0}^{p_{mT}} m_{T,k} \bar{b}_{k+2T}(x) \\ A_{2,3}(x) = -I_T G(x) \sum_{k=0}^{p_{mT}} m_{T,k} \bar{b}'_{k+2T}(x) \end{bmatrix}. \end{aligned} \quad (5)$$

By setting $x = L$ in (5), the dependence of the state variables at point j on the ones at the initial point i is obtained. It reads as

$$\begin{aligned} \begin{bmatrix} \psi_j \\ M_{T,j} \end{bmatrix} &= \begin{bmatrix} A_{1,1}|_{x=L} = \bar{b}_{0T}(x)|_{x=L} & A_{1,2}|_{x=L} = \frac{\bar{b}_{1T}(x)|_{x=L}}{I_T G(x)|_{x=0}} \\ A_{2,1}|_{x=L} = I_T G(x)|_{x=L} \bar{b}'_{0T}(x)|_{x=L} & A_{2,2}|_{x=L} = \frac{I_T G(x)|_{x=L}}{I_T G(x)|_{x=0}} \bar{b}'_{1T}(x)|_{x=L} \end{bmatrix} \cdot \begin{bmatrix} \psi_i \\ M_{T,i} \end{bmatrix} \\ &+ \begin{bmatrix} A_{1,3}|_{x=L} = -\sum_{k=0}^{p_{mT}} m_{T,k} \bar{b}_{k+2T}(x)|_{x=L} \\ A_{2,3}|_{x=L} = -I_T G(x)|_{x=L} \sum_{k=0}^{p_{mT}} m_{T,k} \bar{b}'_{k+2T}(x)|_{x=L} \end{bmatrix}. \end{aligned} \quad (6)$$

By simple mathematical manipulations, the local finite element equation for uniform torsion, where $\bar{M}_{T,i} = -M_{T,i}$ according to the definition of the positive orientation of the state variables – see Fig. 1, is obtained as

$$\begin{aligned}
\begin{bmatrix} \bar{M}_{T,i} \\ M_{T,j} \end{bmatrix} &= \begin{bmatrix} B_{1,1} = \frac{A_{1,1}|_{x=L}}{A_{1,2}|_{x=L}} & B_{1,2} = -\frac{1}{A_{1,2}|_{x=L}} \\ B_{2,1} = A_{2,1}|_{x=L} - \frac{A_{1,1}|_{x=L} A_{2,2}|_{x=L}}{A_{1,2}|_{x=L}} & B_{2,2} = \frac{A_{2,2}|_{x=L}}{A_{1,2}|_{x=L}} \end{bmatrix} \begin{bmatrix} \psi_i \\ \psi_j \end{bmatrix} \\
&+ \begin{bmatrix} F_1 = \frac{A_{1,3}|_{x=L}}{A_{1,2}|_{x=L}} \\ F_2 = A_{2,3}|_{x=L} - \frac{A_{1,3}|_{x=L} A_{2,2}|_{x=L}}{A_{1,2}|_{x=L}} \end{bmatrix}.
\end{aligned} \tag{7}$$

The transfer constants $[\bar{b}_{kT}]_{x=L}$ and $[\bar{b}'_{kT}]_{x=L}$, ($k \in \langle 0, p_{mx} + 2 \rangle$), can be calculated with the help of a simple numerical algorithm [21], which was programmed by the authors of [23], using the software MATHEMATICA [22]. The beam element matrix \mathbf{B} is symmetric.

2.2 Eigenvibrations due to non-uniform torsion (warping eigenvibrations)

Fig. 2 refers to determination of the eigenvibrations due to non-uniform torsion. It shows the torsional moment $M_T(x)$, representing the sum of the primary torsional moment $M_{Tp}(x)$ and the secondary torsional moment $M_{Ts}(x)$, and the bimoment $M_\omega(x)$ according to the formulation in the framework of the transfer matrix method (TMM). Fig. 2 also shows the angle of twist $\psi(x)$, corresponding to $M_{Tp}(x)$. It represents the sum of the angle of twist, resulting from the primary deformation, $\psi'_M(x)$, and from the secondary deformation, $\psi'_S(x)$.

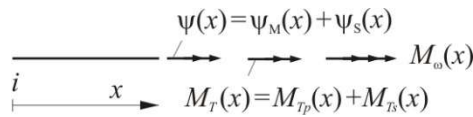


Fig. 2: Non-uniform torsion: torsional moments, bimoment, and angles of twist.

Fig. 3 illustrates the beam element. It is loaded by the equivalent inertial torsional line moment $\omega^2 I_p \rho(x) \psi(x)$, the equivalent inertial line bimoment $\omega^2 I_\omega \rho(x) \psi'_M(x)$, where I_ω stands for the warping constant, and the torsional line moment $m_T(x)$, which is equal to zero for modal analysis. These line moments represent the static equivalent of the respective dynamic action. In the following, the equilibrium equations will be formulated. They are obtained as

$$M'_T(x) = -m_T(x) - \omega^2 I_p \rho(x) \psi(x), \tag{8}$$

where $m_T(x) = \sum_{k=0}^{\max k} \eta_{m_T,k} x^k$ is the polynomial representation of the torsion moment with the parameters $\eta_{m_T,k}$, and

$$\begin{aligned} M'_\omega(x) &= M_T(x) - M_{Tp}(x) + m_\omega(x) + \omega^2 I_\omega \rho(x) \psi'_M(x) = \\ &= M_{Ts}(x) + m_\omega(x) + \omega^2 I_\omega \rho(x) \psi'_M(x), \end{aligned} \quad (9)$$

where $m_\omega(x) = \sum_{k=0}^{\max k} \eta_{m_\omega,k} x^k$ is the polynomial representation of the warping moment with the parameters $\eta_{m_\omega,k}$, and

$$M_T(x) = M_{Tp}(x) + M_{Ts}(x). \quad (10)$$

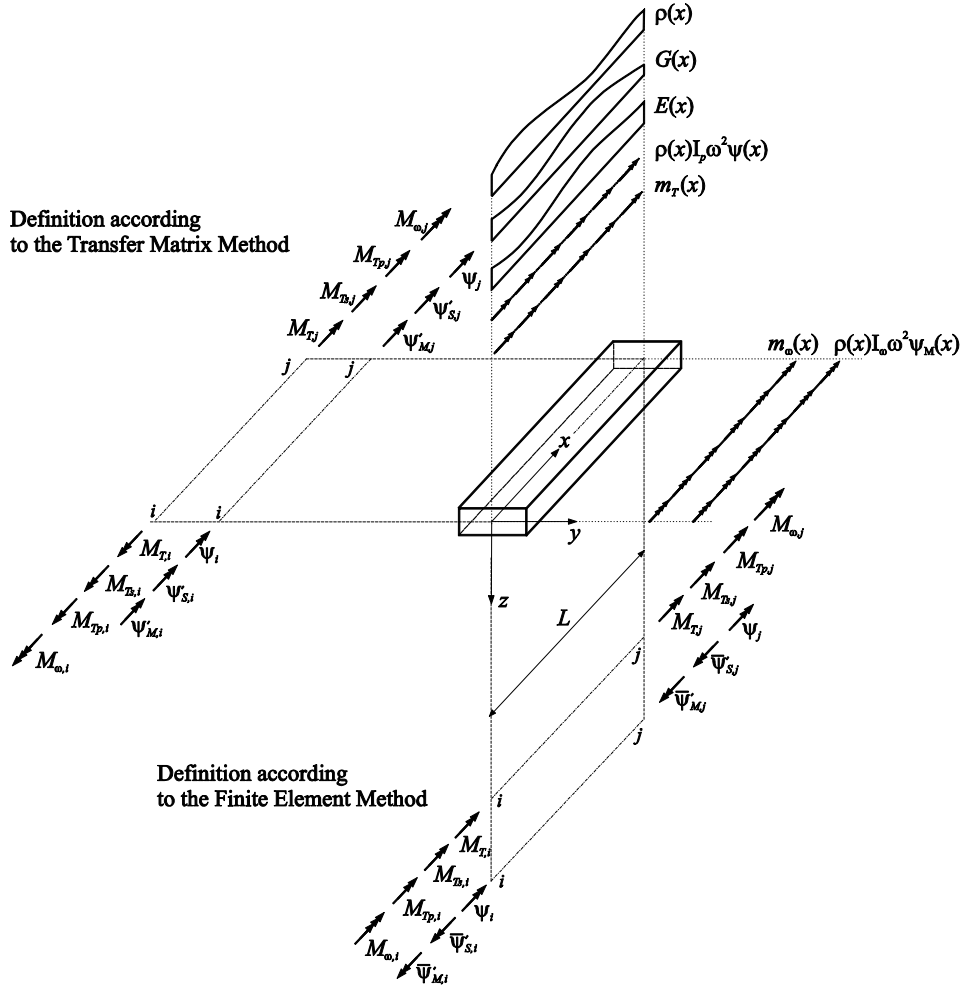


Fig. 3: Positive orientation of the moments and rotation angles at element nodes for the TMM and the FEM.

According to [1],

$$\psi''_M(x) = -\frac{M_\omega(x)}{E(x)I_\omega} \quad (11)$$

and

$$\psi'(x) = \psi'_M(x) + \psi'_S(x) \quad (12)$$

with

$$\psi'_M(x) = \frac{M_{Tp}(x)}{G(x)I_T} \quad (13)$$

and

$$\psi'_S(x) = \frac{M_{Ts}(x)}{G(x)I_{Ts}}, \quad (14)$$

where I_{Ts} denotes the secondary torsion constant and $E(x)$ and $G(x)$ stand for the longitudinally varying effective elasticity modulus and shear modulus, respectively. The new polynomial $G(x)I_{Ts}$ is obtained by multiplication of the secondary torsion constant I_{Ts} with the polynomial for the shear modulus, $G(x)$.

The polynomial $E(x)I_\omega$ is obtained by multiplication of the warping constant I_ω with the polynomial representation of Young's modulus, $E(x)$.

Differentiation of (14) with respect to x and multiplication by $I_\omega E(x)$ gives

$$M_\omega + \frac{EI_\omega (M_{Ts} G' I_{Ts} + G I_{Ts} (-M'_{Ts} + G I_{Ts} \psi''))}{(G I_{Ts})^2} = 0. \quad (15)$$

Differentiation of (15) with respect to x , multiplication by $(EI_\omega)^2$, and use of (14) yields

$$\left. \begin{aligned} & \left(-2EI_\omega M_{Ts} (G' I_{Ts})^2 + G' I_{Ts} (G I_{Ts} (E' I_\omega M_{Ts} + 2EI_\omega M'_{Ts}) + EI_\omega M_{Ts} G'' I_{Ts}) \right) \\ & \frac{(EI_\omega)^2}{(G I_{Ts})^3} \left(- (G I_{Ts})^2 (\omega^2 I_\omega \rho M_{Ts} + E' I_\omega M'_{Ts} + EI_\omega M''_{Ts}) \right. \\ & \left. + (EI_{Ts})^3 (M_{Ts} + m_\omega + \omega^2 I_\omega \rho \psi' + E' I_\omega \psi'' + EI_\omega \psi''') \right) \end{aligned} \right) = 0. \quad (16)$$

According to (13), M_{Tp} is inserted into (10). After some mathematical manipulations, this yields

$$M_{Ts} = M_T - M_{Tp} = M_T - G I_T \psi'. \quad (17)$$

The first and the second derivative of (17) with respect to x is substituted into (16), and the torsion moment is expressed as

$M_T \left((GI_{Ts})^3 - (GI_{Ts})^2 \omega^2 I_{\omega} \rho + GI_{Ts} E'I_{\omega} G'I_{Ts} - 2EI_{\omega} (G'I_{Ts})^2 + EI_{\omega} GI_{Ts} G''I_{Ts} \right) =$	
$+ \left(2I_p \omega^2 \rho EI_{\omega} GI_{Ts} G'I_{Ts} - \omega^2 I_p \rho (GI_{Ts})^2 E'I_{\omega} - \omega^2 I_{\omega} \rho' EI_{\omega} (GI_{Ts})^2 \right)$	$\cdot \psi$
$+ (GI_T (GI_{Ts})^3 - \omega^2 I_p \rho EI_{\omega} (GI_{Ts})^2 - \omega^2 I_{\omega} \rho GI_T (GI_{Ts})^4 - \omega^2 I_{\omega} \rho (GI_{Ts})^3 (GI_T (GI_{Ts})^3$ $- \omega^2 I_p \rho EI_{\omega} (GI_{Ts})^2 - \omega^2 I_{\omega} \rho GI_T (GI_{Ts})^2 - \omega^2 I_{\omega} \rho (GI_{Ts})^3 - (GI_{Ts})^2 E'I_{\omega} G'I_T$ $+ GI_T GI_{Ts} E'I_{\omega} G'I_{Ts} + 2EI_{\omega} GI_{Ts} G'I_T G'I_{Ts} - 2EI_{\omega} GI_T (G'I_{Ts})^2$ $- EI_{\omega} (GI_{Ts})^2 G''I_T + EI_{\omega} GI_T GI_{Ts} G''I_{Ts})$	$\cdot \psi'$
$+ \left(2EI_{\omega} GI_T GI_{Ts} G'I_{Ts} - GI_T (GI_{Ts})^2 E'I_{\omega} - (GI_{Ts})^3 E'I_{\omega} - 2EI_{\omega} (GI_{Ts})^2 G'I_T \right)$	$\cdot \psi''$
$- \left(EI_{\omega} GI_T (GI_{Ts})^2 + EI_{\omega} (GI_{Ts})^3 \right)$	$\cdot \psi'''$
$- (GI_{Ts})^3 m_{\omega} + \left(-E'I_{\omega} (GI_{Ts})^2 + 2EI_{\omega} GI_{Ts} G'I_{Ts} \right) m_T - EI_{\omega} (GI_{Ts})^2 m'_T$	

(18)

The first derivative of (18) is formally established and set equal to $M'_T = -m_T - \omega^2 I_p \rho \psi$. In this way, the following differential equation of fourth order is obtained:

$$\eta_4(x)\psi''''(x) + \eta_3(x)\psi'''(x) + \eta_2(x)\psi''(x) + \eta_1(x)\psi'(x) + \eta_0(x)\psi(x) = \eta_L(x) = \sum_{s=0}^{\max s} \eta_{L,s} x^s \quad (19)$$

The variable polynomial coefficients are given in Appendix A1.

The general semi-analytical solution of the differential equation (19) can be written as follows:

$$\psi(x) = b_0(x)\psi_i + b_1(x)\psi'_i + b_2(x)\psi''_i + b_3(x)\psi'''_i + \sum_{s=0}^{\max s} \eta_{L,s} b_{s+4}(x). \quad (20)$$

In (20), $b_0(x)$, $b_1(x)$, $b_2(x)$, $b_3(x)$, and $b_{s+4}(x)$, $s \in \langle 0, \max s \rangle$ denote the transfer functions and ψ_i , ψ'_i , ψ''_i , ψ'''_i stand for the integration constants of the starting point i , see Figs. 3 and 4, (e.g. $\psi_i = \psi(x)$ for $x=0$, etc...).

(20) and its first three derivatives with respect to x are condensed to the following matrix equation:

$$\begin{bmatrix} \psi(x) \\ \psi'(x) \\ \psi''(x) \\ \psi'''(x) \end{bmatrix} = \begin{bmatrix} b_0(x) & b_1(x) & b_2(x) & b_3(x) \\ b'_0(x) & b'_1(x) & b'_2(x) & b'_3(x) \\ b''_0(x) & b''_1(x) & b''_2(x) & b''_3(x) \\ b'''_0(x) & b'''_1(x) & b'''_2(x) & b'''_3(x) \end{bmatrix} \begin{bmatrix} \psi_i \\ \psi'_i \\ \psi''_i \\ \psi'''_i \end{bmatrix} + \begin{bmatrix} \sum_{s=0}^{\max s} \eta_{Ls} b_{s+4}(x) \\ \sum_{s=0}^{\max s} \eta_{Ls} b'_{s+4}(x) \\ \sum_{s=0}^{\max s} \eta_{Ls} b''_{s+4}(x) \\ \sum_{s=0}^{\max s} \eta_{Ls} b'''_{s+4}(x) \end{bmatrix} \cdot \psi^L \quad (21)$$

Then, the load vector, and the matrix \mathbf{b} in (21) are established:

$$\begin{bmatrix} \psi \\ \psi(x) \\ \psi'(x) \\ \psi''(x) \\ \psi'''(x) \\ \hline 1 \end{bmatrix} = \begin{bmatrix} b_0(x) & b_1(x) & b_2(x) & b_3(x) & \sum_{s=0}^{\max s} \eta_{Ls} b_{s+4}(x) \\ b'_0(x) & b'_1(x) & b'_2(x) & b'_3(x) & \sum_{s=0}^{\max s} \eta_{Ls} b'_{s+4}(x) \\ b''_0(x) & b''_1(x) & b''_2(x) & b''_3(x) & \sum_{s=0}^{\max s} \eta_{Ls} b''_{s+4}(x) \\ b'''_0(x) & b'''_1(x) & b'''_2(x) & b'''_3(x) & \sum_{s=0}^{\max s} \eta_{Ls} b'''_{s+4}(x) \\ \hline 0 & 0 & 0 & 0 & 1 \end{bmatrix} \begin{bmatrix} \psi_i \\ \psi'_i \\ \psi''_i \\ \psi'''_i \\ \hline 1 \end{bmatrix}, \quad (22)$$

In (22), \mathbf{b} is a matrix, containing the solution functions of the differential equation (20) and of their first three derivatives at x (the so-called transfer functions for torsion with warping), ψ is a vector containing the angle of twist and its first three derivatives at x , and ψ_i is a vector containing the values of the angle of twist and its first three derivatives at the starting point i , and ψ^L is a load vector. Based on the dependence of $\psi'(x)$, $\psi''(x)$, and $\psi'''(x)$ on $M_T(x)$ and $M_\omega(x)$, the transfer matrix expression (24) is obtained.

The transfer matrix \mathbf{A} relates the “static vector” \mathbf{Z}_i to the vector \mathbf{Z}_x .

$$\begin{bmatrix} \mathbf{Z}_x \\ \psi(x) \\ \psi'_M(x) \\ M_\omega(x) \\ M_T(x) \\ \hline 1 \end{bmatrix} = \begin{bmatrix} A_{1,1}(x) & A_{1,2}(x) & A_{1,3}(x) & A_{1,4}(x) & A_{1,5}(x) \\ A_{2,1}(x) & A_{2,2}(x) & A_{2,3}(x) & A_{2,4}(x) & A_{2,5}(x) \\ A_{3,1}(x) & A_{3,2}(x) & A_{3,3}(x) & A_{3,4}(x) & A_{3,5}(x) \\ A_{4,1}(x) & A_{4,2}(x) & A_{4,3}(x) & A_{4,4}(x) & A_{4,5}(x) \\ \hline 0 & 0 & 0 & 0 & 1 \end{bmatrix} \begin{bmatrix} \mathbf{Z}_i \\ \psi_i \\ \psi'_{M,i} \\ M_{\omega,i} \\ M_{T,i} \\ \hline 1 \end{bmatrix}. \quad (23)$$

A detailed description of these terms is given in Appendix A2.

The kinematic and kinetic variables at node i are denoted by the index i in (23). By setting $x = L$ in this relation, the dependence of the nodal variables at node j on the

nodal variables at node i is obtained. Then, using appropriate mathematical operations, the local finite element equations for non-uniform torsion (in particular for free torsional vibrations) read as follows (considering the definitions of positive quantities in the framework of the FEM, resulting in $\bar{M}_{T,i} = -M_{T,i}$, $\bar{M}_{\omega,i} = -M_{\omega,i}$, $\bar{\psi}'_{M,i} = -\psi'_{M,i}$, and $\bar{\psi}'_{M,j} = -\psi'_{M,j}$):

$$\begin{bmatrix} \bar{M}_{T,i} \\ \bar{M}_{\omega,i} \\ M_{T,j} \\ M_{\omega,j} \end{bmatrix} = \begin{bmatrix} B_{1,1} & B_{1,2} & B_{1,3} & B_{1,4} \\ B_{2,1} & B_{2,2} & B_{2,3} & B_{2,4} \\ B_{3,1} & B_{3,2} & B_{3,3} & B_{3,4} \\ B_{4,1} & B_{4,2} & B_{4,3} & B_{4,4} \end{bmatrix} \cdot \begin{bmatrix} \psi_i \\ \bar{\psi}'_{M,i} \\ \psi_j \\ \bar{\psi}'_{M,j} \end{bmatrix} + \begin{bmatrix} F_1 \\ F_2 \\ F_3 \\ F_4 \end{bmatrix}, \quad (24)$$

A detailed description of the matrix coefficients in (24) is presented in Appendix A3.

The local finite element matrix \mathbf{B} in (25) is symmetric. It consists of the stiffness matrix \mathbf{K} and the consistent mass matrix \mathbf{M} :

$$[\mathbf{B}] = [\mathbf{K} - \omega^2 \mathbf{M}]. \quad (25)$$

For a structure consisting of straight beams, the global structural matrix is obtained by assembling the element matrices according to standard FEM technology. Since the TMM does not allow for analyzing frames, FE analysis of frames would not be particularly useful, since the results could not be compared with results from other methods.

In modal analysis, an eigenvalue problem must be solved. For given longitudinally varying effective material properties and global boundary conditions, the value of the circular frequency ω is increased until the determinant of the global system matrix becomes zero. The respective circular frequency is the natural circular frequency, from which the natural frequency (eigenfrequency) can be calculated. Further, the mode shape can be calculated by the transfer relations (23), by considering the first line without the load term.

The described solution algorithm was implemented into MATHEMATICA [22]. The eigenfrequencies were calculated for selected cantilever beams with thin-walled open and closed cross-sections. In Chapter 3, the results of the numerical experiments are presented and compared with the results obtained from the available commercial software.

3. Numerical investigation

In this Chapter, modal analysis of cantilever FGM beams with an I-cross-section and a hollow cross-section of length $L = 0.1$ m is performed. The FGM consists of a mixture of aluminum (denoted with the index m) and tungsten (denoted with the index f). The material properties are shown in Table 1.

Material properties:		
Young's modulus	$E_f = 4.8 \cdot 10^{11}, E_m = 0.69 \cdot 10^{11}$	Pa
Poisson's ratio	$\nu_f = 0.2, \nu_m = 0.33$	-
Shear modulus	$G_f = 2.0 \cdot 10^{11}, G_m = 0.26 \cdot 10^{11}$	Pa
Mass density	$\rho_f = 4920, \rho_m = 2700$	kg/m ³

Table 1: Material properties of the FGM constituents.

The longitudinal polynomial variation of the effective Young's modulus (26) and the effective Poisson's ratio (27) is assumed as:

$$E(x) = E_f + (E_m - E_f) \left(\frac{x}{L} \right)^n, \quad (26)$$

$$\nu(x) = \nu_f + (\nu_m - \nu_f) \left(\frac{x}{L} \right)^n, \quad (27)$$

Despite the rather academic nature of these material properties, they allow for determination of the effect of their variability on the eigenvibrations of thin-walled beams, considering the influence of non-uniform torsion.

In (26) and (27), n is the order of the polynomial. The effective shear modulus reads as:

$$G(x) = \frac{E(x)}{2(1+\nu(x))}. \quad (28)$$

The effective mass density is chosen as

$$\rho(x) = \rho_f + (\rho_m - \rho_f) \left(\frac{x}{L} \right)^n. \quad (29)$$

The longitudinal beam axis x begins at the clamped end of the cantilever beam ($x = 0$). The axial variations of the material properties are shown in Figs. 4 and 5 for $n \in \langle 1, 5 \rangle$.

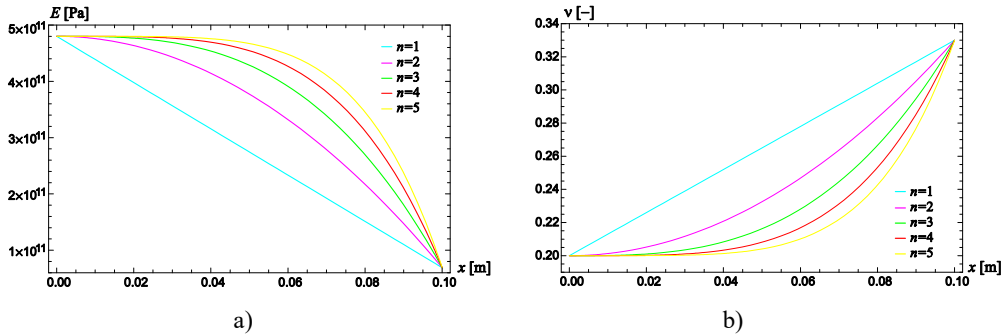


Fig. 4: Variation of a) Young's modulus and b) Poisson's ratio.

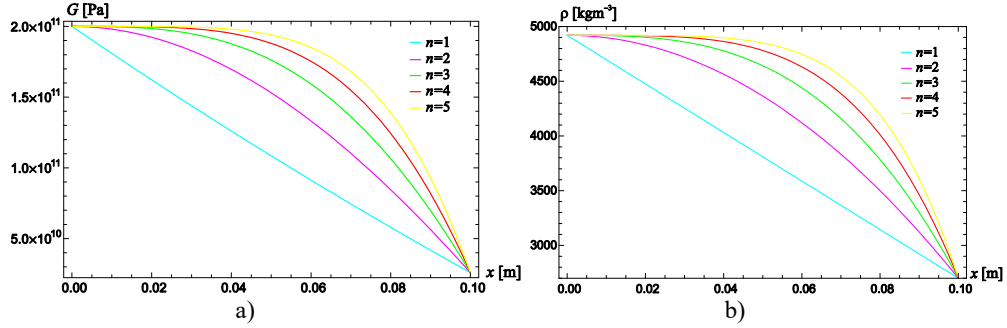


Fig. 5: Variation of a) shear modulus and b) mass density.

3.1 Eigenfrequencies and mode shapes of a cantilever beam with an I cross-section, with longitudinally varying material properties

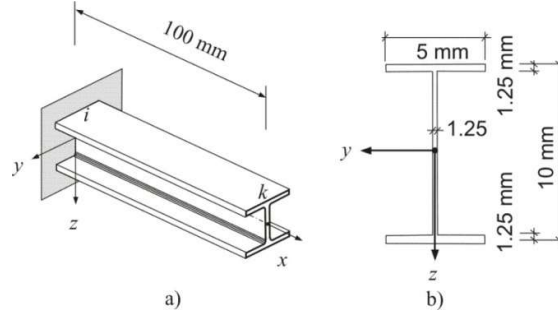


Fig. 6: Cantilever beam with an I cross-section a) system, b) cross-section.

The cross-sectional dimensions of the cantilever beam of length $L = 0.1$ m, shown in Fig. 6, are given as $h = 0.01$ m, $b = 0.005$ m, $t = s = 0.00125$ m. In Table 2, the required cross-sectional parameters are listed. The geometric constants in Table 2 are computed by means of ANSYS [3], except the secondary torsion constant and the warping torsion constant, which were calculated by means of Thin Tube Theory [25].

Cross-sectional parameters [3], [25]		
Cross-sectional area	$A = 0.21875 \cdot 10^{-4}$	m ²
Second moment of area about the y -axis	$I_y = 0.28483 \cdot 10^{-9}$	m ⁴
Second moment of area about the z -axis	$I_z = 0.27262 \cdot 10^{-10}$	m ⁴
Polar moment of area	$I_p = I_y + I_z = 0.31212 \cdot 10^{-9}$	m ⁴
Torsion constant	$I_T = 0.1119 \cdot 10^{-10}$	m ⁴
Secondary torsion constant	$I_{Ts} = 0.19938 \cdot 10^{-9}$	m ⁴
Warping constant	$I_\omega = 0.498 \cdot 10^{-15}$	m ⁶

Table 2: Cross-sectional parameters for warping torsion.

The first three Saint-Venant torsional and warping eigenfrequencies were calculated for the considered cantilever beam.

For modal analysis, the following boundary conditions were specified:

a) Saint-Venant torsional vibrations (according to Subchapter 2.1):

$$\psi(x)|_{x=0} = \psi_i = 0, \quad M_T(x)|_{x=L} = M_{T,k} = 0. \quad (30)$$

b) Warping vibrations (according to Subchapter 2.2):

$$\begin{aligned} \psi(x)|_{x=0} = \psi_i = 0, \quad \psi'_M(x)|_{x=0} = \psi'_{M,i} = 0, \\ M_\omega(x)|_{x=L} = M_{\omega,k} = 0, \quad M_T(x)|_{x=L} = M_{T,k} = 0. \end{aligned} \quad (31)$$

Important remark: According to the analogy between non-uniform torsion and the Timoshenko beam theory [25], the following conditions hold at the clamped end of the beam:

for the case of flexural vibrations: $\frac{\partial w}{\partial x}|_{x=0} = w'_i \neq 0$, but $\varphi|_{x=0} = \varphi_i = 0$, and

for the case of warping vibrations: $\frac{\partial \psi}{\partial x}|_{x=0} = \psi'_i \neq 0$, but $\frac{\partial \psi'_M}{\partial x}|_{x=0} = \psi'_{M,i} = 0$,

where $w = w(x)$ is the deflection and $\varphi = \varphi(x)$ is the angle of rotation of the cross-section about the y-axis.

For determination of the warping vibrations, taking the boundary conditions into account, a reduced system of two homogeneous algebraic equations with the unknowns $M_\omega(x)|_{x=0} = M_{\omega,i}$ and $M_T(x)|_{x=0} = M_{T,i}$ is obtained.

The first three torsional eigenfrequencies were calculated by

a) one warping torsion finite beam element (WT), simplified for Saint-Venant torsion (SV), one warping torsion finite beam element with STMDE (WT - with STMDE), and for warping torsion without STMDE (WT-without STMDE).

b) a very fine mesh of 3D solid finite elements of the commercial software ABAQUS [5] - (258000 finite elements) and ANSYS [3] - (7560/16000/105000 SOLID186 elements). The results are shown in Table 3.

f [Hz]	n	SV	WT - with STMDE	WT - without STMDE	ANSYS SOLID186	ABAQUS
1	1	3003.1	3217.5	3287.4	3346.8/3332.5/3329.6	3368.5
	2	3422.5	3502.5	3614.2	3625.1/3609.7/3606.7	3614.2
	3	3287.5	3560.4	3706.4	3686.3/3670.9/3667.9	3675.8
	4	3227.4	3553.0	3729.8	3690.4/3675.0/3672.0	3679.5
	5	3208.6	3524.4	3731.4	3678.4/3663.2/3660.2	3667.6
	1	7369.7	8444.9	8699.7	8799.3/8768.4/8762.5	8832.2
	2	7683.0	9171.4	9648.3	9639.6/9605.6/9599.7	9617.1

2	3	8531.1	9510.1	10208.7	10120.1/10084.8/10078.5	10097.0
	4	8800.1	9682.8	10587.6	10434.4/10398.1/10391.7	10411.0
	5	8970.7	9760.7	10853.4	10647.4/10610.4/10604.0	10624.0
3	1	11979.2	15440.3	15920.0	16025.7/15986.9/15979.7	16074.0
	2	16017.2	16557.3	17440.3	17479.8/17438.4/17431.1	17454.0
	3	13768.5	16982.5	18273.7	18260.0/18217.5/18210.5	18235.0
	4	14172.6	17149.8	18828.1	18753.4/18710.4/18703.7	18729.0
	5	14451.5	17198.5	19234.1	19092.4/19048.9/19042.5	19069.0

Table 3: Eigenfrequencies calculated by WT and 3D solid finite elements with material properties for $n \in \langle 1, 5 \rangle$ according to Figs. 5 and 6.

Plots of the dependence of the first eigenfrequency on the order n of the polynomial, describing the longitudinal variation of the material properties, are shown in Fig. 8. The dependence of the 1st eigenfrequency on the number of SOLID186 finite elements is shown in Fig. 8.

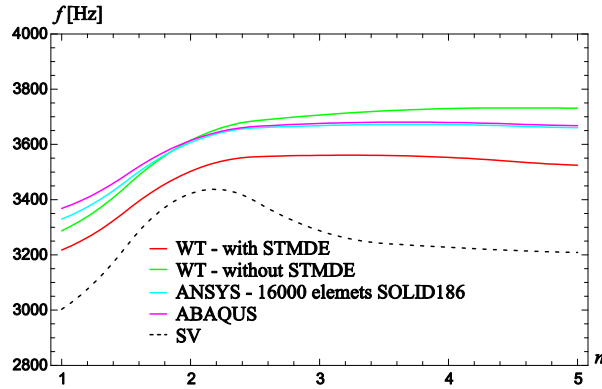


Fig. 7: Dependence of the 1st eigenfrequency on the order n in (26), (27), and (29).

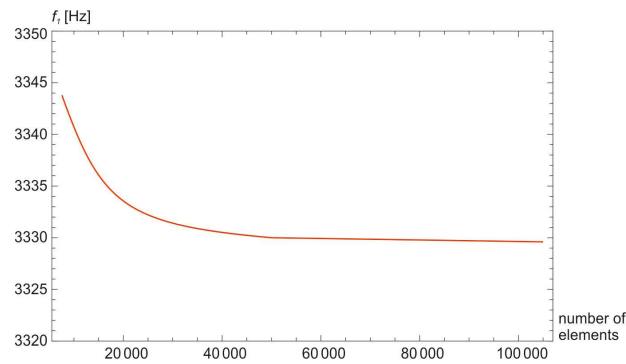


Fig. 8: Dependence of the 1st eigenfrequency on the number of BEAM186 elements.

As shown in Table 3 and Fig. 7, the best agreement of the results with 3D solid finite elements is obtained by the warping torsion finite beam element without consideration STDME for all of the investigated beams. Consideration of STMDE results in a decrease of the torsional stiffness. The difference from the benchmark solution

becomes notable for the higher modes. As expected, the Saint-Venant solution (SV) is characterized by unsuitable results. It is also shown that the variation of the material properties has a significant influence on the results.

The same example was solved with BEAM188 finite elements [3], with the following options: warping unrestrained (WU) and warping restrained (WR). A very fine mesh with 100 BEAM188 finite beam elements was used. The relevant material properties were assigned to each element according to the variations shown in Figs. 4 and 5. The obtained results are listed in Table 4.

f [Hz]	n	BEAM188 WU	BEAM188 WR	WT - with STMDE	WT - without STMDE	SOLID186 105000 FE
1	1	3086.9	3343.3	3217.5	3287.4	3329.6
	2	3301.7	3621.7	3502.5	3614.2	3606.7
	3	3329.2	3682.8	3560.4	3706.4	3667.9
	4	3317.3	3686.7	3553.0	3729.8	3672.0
	5	3298.0	3674.6	3524.4	3731.4	3660.2
2	1	7575.8	8873.7	8444.9	8.699.7	8832.2
	2	8331.7	9721.7	9171.4	9648.3	9617.1
	3	8769.6	10205.4	9510.1	10208.7	10097.0
	4	9046.0	10521.1	9682.8	10587.6	10411.0
	5	9221.2	10734.6	9760.7	10853.4	10604.0
3	1	12319.4	16319.0	15440.3	15920.0	16074.0
	2	13504.2	17801.5	16557.3	17440.3	17431.1
	3	14155.6	18597.8	16982.5	18273.7	18235.0
	4	14570.9	19102.1	17149.8	18828.1	18729.0
	5	14857.5	19449.0	17198.5	19234.1	19069.0

Table 4: Eigenfrequencies calculated by BEAM186 finite elements with material properties for $n \in \langle 1,5 \rangle$ - according to Figs. 4 and 5.

Plots of the dependence of the 1st eigenfrequency, computed with BEAM188 and the WT finite beam element, on the order n of the polynomial, describing the variation of the material properties, are shown in Fig. 9.

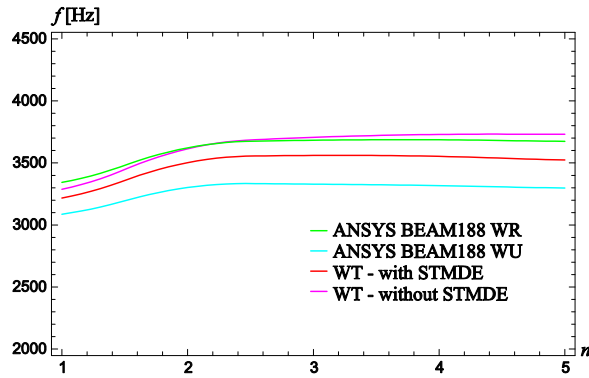


Fig. 9: Dependence of the 1st eigenfrequency on the order n in (26), (27) and (29).

As shown in Table 5 and Fig. 9, the results obtained by BEAM188 WR are very close to the results obtained by only one WT - without STDME finite element, and both agree well with the benchmark solution (by 105000 SOLID186 finite elements). The calculated modes are shown in Fig.10. No distortion of the cross-section occurs in the solved cases.

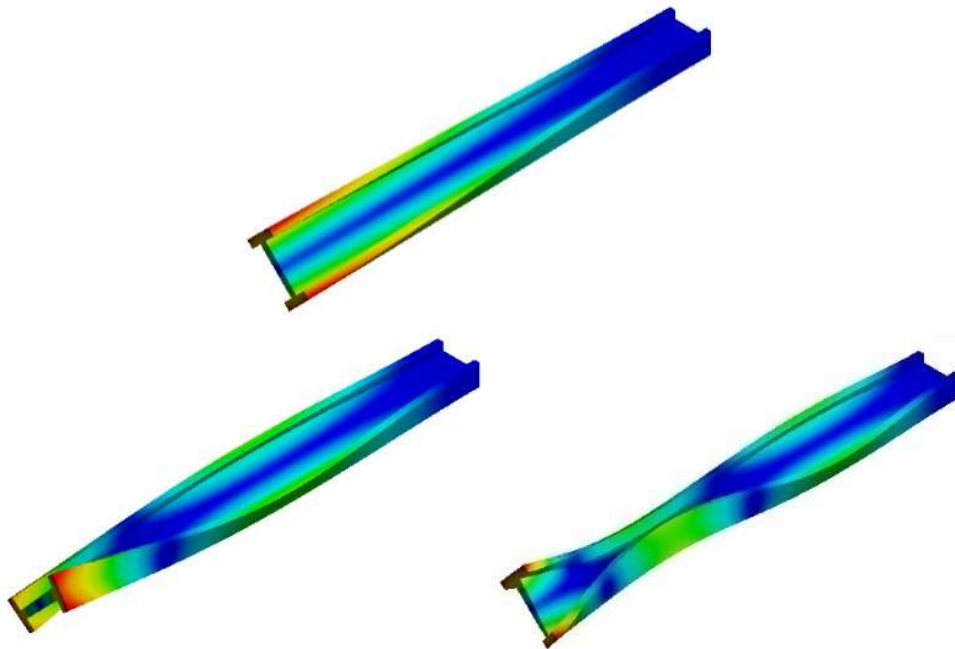


Fig. 10: Mode shapes corresponding to the 1st, 2nd, and 3rd warping torsion eigenfrequency [3].

3.2 Warping eigenfrequencies and mode shapes of a cantilever beam with a rectangular hollow cross-section, with longitudinally varying material properties.

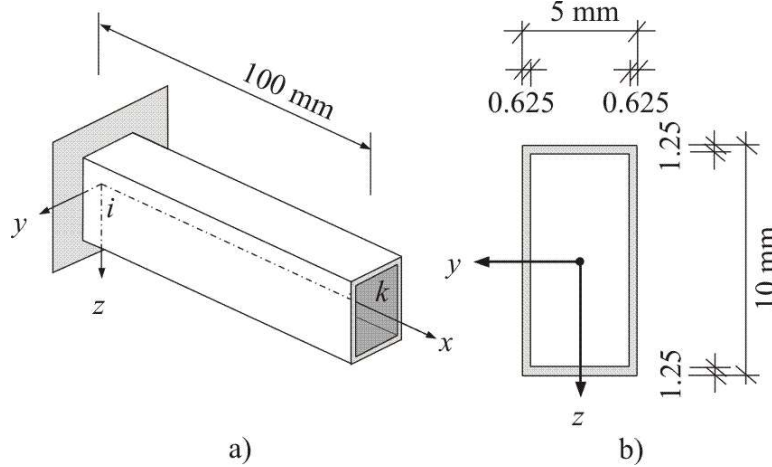


Fig. 11: Cantilever beam with a rectangular hollow cross-section: a) system, b) cross-section.

The cross-sectional parameters including the mechanical characteristics are calculated by ANSYS [3] and TTT [25]. They are listed in Table 5.

Cross-sectional parameters [3], [25]		
Cross-sectional area	$A = 0.21875 \cdot 10^{-4}$	m ²
Second moment of area about the y -axis	$I_y = 0.71208 \cdot 10^{-10}$	m ⁴
Second moment of area about the z -axis	$I_z = 0.28483 \cdot 10^{-9}$	m ⁴
Polar moment of area	$I_p = I_y + I_z = 0.31209 \cdot 10^{-9}$	m ⁴
Torsion constant	$I_T = 0.16748 \cdot 10^{-9}$	m ⁴
Secondary torsion constant	$I_{Ts} = 0.717773 \cdot 10^{-10}$	m ⁴
Warping constant	$I_\omega = 0.240426 \cdot 10^{-15}$	m ⁶

Table 5: Cross-sectional parameters of the hollow cross-section.

The material characteristics are listed in Table 1. The boundary conditions are the same as in Chapter 3, (26) and (29).

The aim of this investigation is to evaluate the influence of warping and of the variation of the material properties on the eigenfrequencies of beams with closed cross-sections, with longitudinally varying material properties according to Figs. 4 and 5.

The first three torsional eigenfrequencies were calculated by

- only one warping torsion finite element (WT) for Saint-Venant torsion (SV), for warping torsion with STMDE (WT - with STMDE), and for warping torsion without STMDE (WT-without STMDE).

b) a very fine mesh of 3D solid finite elements of the commercial software ABAQUS [5] (258000 finite elements) and ANSYS [3] (26100/100800 SOLID186 elements). The results are shown in Table 6.

f [Hz]	n	SV	WT - with STMDE	WT - without STMDE	ANSYS SOLID186	ABAQUS
1	1	11345.9	10911.7	11422.5	11026.1/11021.3	11130.0
	2	12135.6	11663.1	12239.9	11846.4/11841.5	11857.0
	3	12236.8	11746.0	12342.7	11993.3/11988.6	12003.0
	4	12193.1	11683.8	12292.0	11981.5/11977.1	11991.0
	5	12122.1	11592.2	12212.3	11931.9/11927.6	11941.0
2	1	27843.1	26822.7	28425.7	22141.2/22099.8	22258.0
	2	30621.3	29346.7	31250.5	24063.3/24017.6	24145.0
	3	32230.9	30755.4	32796.4	25337.0/25289.2	25420.0
	4	33247.1	31617.3	33743.0	26267.8/26218.9	26351.0
	5	33891.3	32503.1	34329.7	26957.2/26908.0	27040.0
3	1	45257.7	43799.2	46516.4	29200.2/29147.1	29316.0
	2	49623	47713.3	51033.5	31667.4/31610.8	31772.0
	3	52017.4	49719.3	53402.3	32963.3/32903.3	33070.0
	4	53544.2	50907.7	54856.3	33774.3/33711.3	33884.0
	5	54597.8	51663.6	55822.4	34342.4/34276.8	34454.0

Table 6: Eigenfrequencies calculated by WT and 3D solid finite elements with material properties for $n \in \langle 1, 5 \rangle$ according to Figs. 5 and 6.

Plots of the dependence of the 1st eigenfrequency on the order n of the polynomial describing the longitudinal variation of the material properties are shown in Fig. 12.

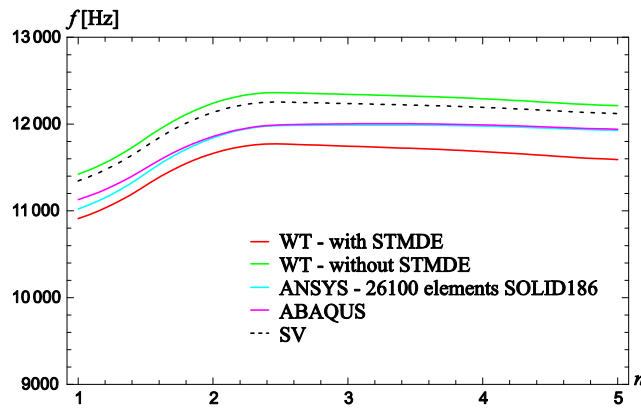


Fig. 12: Dependence of the 1st eigenfrequency on the order n in (26), (27), and (29).

As shown in Table 6 and Fig. 12, the ANSYS and ABAQUS solid finite elements produce consistent results, which were considered as benchmark solutions. Comparable results by the warping finite element (WT - with and without STMDE) are only obtained for the first eigenfrequency. A significant difference occurs for the higher modes. This is likely caused by the incorrect stiffness of the cross-section by the approach on which the WT finite elements are based. It is characterized by computation of the warping constant for hollow cross-sections without consideration of the distortion effect). In reality, the stiffness is influenced not only by warping but also by the distortion of the cross-section [24]. This is shown by the eigenmodes in Fig. 13, calculated by the BEAM186 solid finite elements [3]. As expected, the results are characterized by a significant influence of the variation of the material properties.

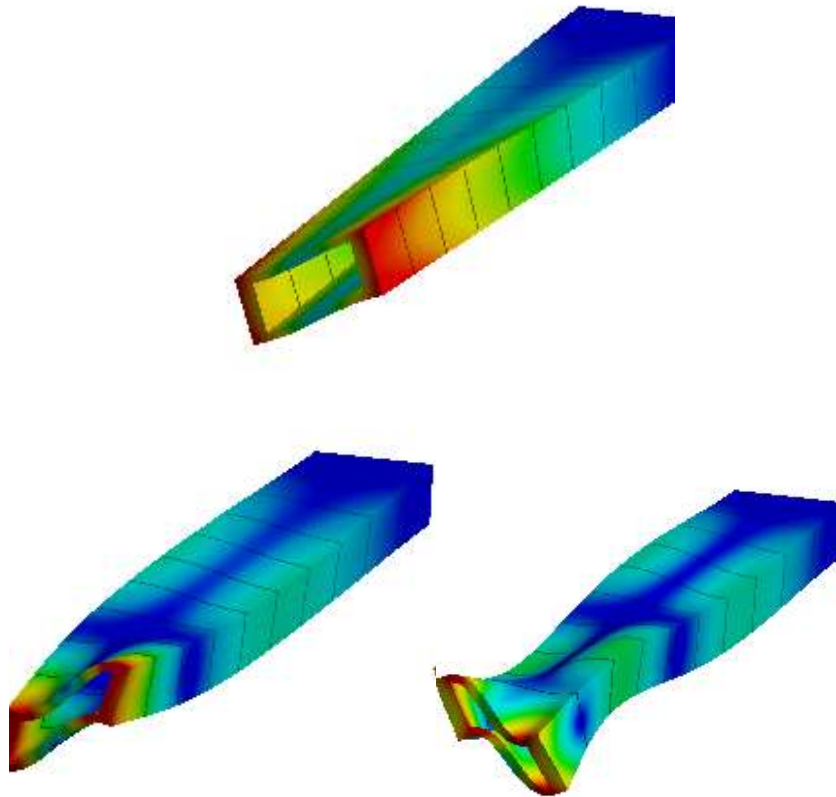


Fig. 13: Mode shapes corresponding to the 1st, 2nd, and 3rd warping torsion eigenfrequency [3].

The same example was solved by means of 100 BEAM188 finite elements [3] with the following options: warping unrestrained (WU) and warping restrained (WR). The results are shown in Table 7.

f [Hz]	n	BEAM188 WU	BEAM188 WR	WT - with STMDE	WT - without STMDE	ANSYS 100860 FE SOLID186
1	1	11346.1	11472.5	10911.7	11422.5	11021.3
	2	12135.7	12309.2	11663.1	12239.9	11857.0
	3	12237.0	12429.0	11746.0	12342.7	12003.0
	4	12193.3	12391.8	11683.8	12292.0	11991.0
	5	12122.2	12322.6	11592.2	12212.3	11941.0
2	1	27845.8	28296.2	26822.7	28425.7	22258.0
	2	30624.0	31136.9	29346.7	31250.5	24145.0
	3	32233.6	32775.2	30755.4	32796.4	25420.0
	4	33249.6	33815.7	31617.3	33743.0	26351.0
	5	33893.8	34482.0	32503.1	34329.7	27040.0
3	1	45270.5	46348.9	43799.2	46516.4	29316.0
	2	49636.4	50818.7	47713.3	51033.5	31772.0
	3	52030.6	53261.2	49719.3	53402.3	33070.0
	4	53557.0	54821.1	50907.7	54856.3	33884.0
	5	54610.5	55900.7	51663.5	55822.4	34454.0

Table 7: Eigenfrequencies calculated by BEAM188 finite elements with material properties for $n \in \langle 1, 5 \rangle$ according to Figs. 4 and 5.

Plots of the dependence of the first eigenfrequency, determined with BEAM188 elements as well as with 100 WT beam finite elements, on the order of the polynomial, describing the longitudinal variation of the material properties, are shown in Fig. 14.

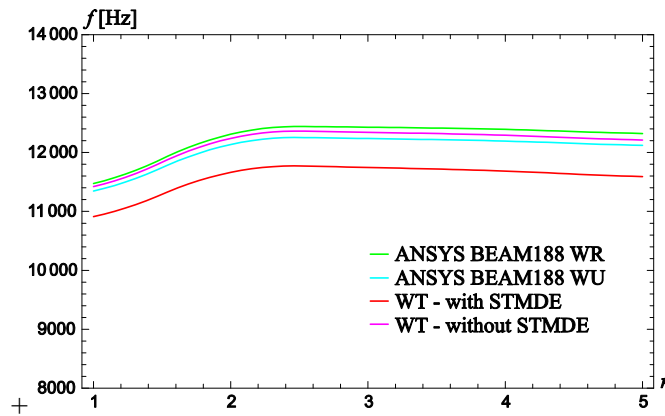


Fig. 14: Dependence of the 1st eigenfrequency on the order n in (26), (27) and (29).

As shown in Table 7 and Fig. 14, consideration of the STMDE in the proposed method improves the accuracy of the results. However, as previously shown, all finite beam elements produce markedly higher eigenfrequencies as compared to the benchmark solution. Except for the 1st eigenfrequency, as regards the modes, the distortion of the

cross-section is not considered by the WT finite elements for the case of torsion with warping. As shown in [26], the distortion does not play such a strong role in the analysis of elastostatic warping torsion, unless the deformation of the twisted beam is similar to its first eigenform and the distortion of the hollow cross-section dominates the reduction of the torsional stiffness.

4. Summary and Conclusions

The differential equations of second order for Saint Venant torsional eigenvariations and of fourth order for non-uniform torsional eigenvariations of FGM beams with doubly symmetric thin-walled open and closed cross-section were established. A polynomial longitudinal continuous variation of the effective material properties was considered. It may e.g. be obtained by homogenization of spatially varying material properties [18]. The general semi-analytical solution of the differential equation (19) was presented and the transfer matrix relations were formulated, from which the finite element equations for FGM beams were obtained. Results from modal analysis of open I beams and rectangular hollow cross-sections by the proposed method were presented and compared with results, obtained by commercial FEM codes. In the theoretical investigation, the secondary torsional moment deformation effect (STDME) was taken into account. A part of the expression for the first derivative of the twist angle was chosen as the warping degree of freedom.

The main conclusions that can be drawn from this investigation are as follows:

- (1) Torsional eigenvariations of open I cross-section cantilever FGM beams:
 - The results from modal analysis, using the proposed torsion finite beam elements, concerning non-uniform (WT) and uniform torsion (SV) of FGM beams with open doubly symmetric cross-sections, have shown large differences of the eigenfrequencies. This proves that the warping effect must be taken into account not only for homogeneous beams but also for beams made of FGM.
 - The proposed approach for calculation of non-uniform torsional eigenvariations with and without consideration of STMDE produces slightly different results for the higher modes. Probably, the STMDE results in a decrease of the torsional stiffness of open cross-sections that is greater than in reality. Evidence of this assumption is the fact that the eigenfrequencies, calculated without consideration of STMDE, agree better with the results obtained by 3D solid finite elements.
 - The proposed warping torsion beam finite element is effective, because the FGM beam with a polynomial variation of the material properties can be modelled with only one such finite element. Results obtained by a coarse mesh agree well with results from a very fine mesh of the 3D SOLID186 or the BEAM188 (WR) finite element [3].
 - As expected, the obtained results show a significant influence of the variation of the material properties on the eigenfrequencies.

(2) Torsional eigenvibrations of a FGM cantilever beam with a rectangular hollow cross-section:

- A reasonably good agreement of the results obtained by the proposed warping finite beam element (WT - with and without STMDE) with the ones obtained by 3D elements is restricted to the 1st eigenfrequency. The significant difference of the results for the higher modes is likely caused by the higher stiffness of the cross-section in case of the proposed approach, where the warping constant is calculated for a rectangular undistorted hollow cross-section. In reality, the decrease of the torsional stiffness is not only caused by warping and STMDE, but also by the distortion of the cross-section [24] (see the second and the third eigenmode in Fig. 14). These effects were not considered by the proposed method. As expected a significant influence of variation of the material properties on the eigenfrequencies occurred, also for the hollow cross-sections.

In future work, the scope of the presented torsional warping beam finite elements will be extended for use in non-uniform torsion elastostatic analysis of FGM beams with a spatial variation of the material properties. As shown in [26], wherein the elastostatic second-order warping torsion analysis of beams with constant material properties is described, the obtained results agree very well with the results from finite solid elements. There, the distortion probably does not play such a strong role, unless the deformation of the twisted beam is similar to its first torsional eigenform.

5. Appendices

A1. The variable polynomial coefficients in (19) given as:

$\eta_0(x) =$
$\begin{aligned} & \omega^2(-\rho I_p - (((GI_{Ts})^3 - \omega^2(GI_{Ts})^2 \rho I_\omega - 2EI_\omega (GI_{Ts})^2 + GI_{Ts} (EI_\omega GI_{Ts} + EI_\omega G''I_{Ts})) \\ & (-GI_{Ts})^2 (2EI_\omega \rho' I_p + \rho I_p E''I_\omega) + EI_\omega (2\rho I_p ((GI_{Ts})^2 + GI_{Ts} G''I_{Ts}) - (GI_{Ts})^2 \rho''' I_p)) \\ & + GI_{Ts} (-2EI_\omega \rho I_p GI_{Ts} + GI_{Ts} (\rho I_p E'I_\omega + EI_\omega \rho' I_p)) ((GI_{Ts})^2 (3GI_{Ts} - \omega^2 \rho' I_\omega) \\ & - GI_{Ts} (EI_\omega G''I_{Ts} + 3EI_\omega G''I_{Ts}) + GI_{Ts} (GI_{Ts} (-2\omega^2 \rho I_\omega + E''I_\omega) + 2EI_\omega G''I_{Ts} + EI_\omega G'''I_{Ts}))) \\ & / (((GI_{Ts})^3 - \omega^2(GI_{Ts})^2 \rho I_\omega - 2EI_\omega (GI_{Ts})^2 + GI_{Ts} (EI_\omega GI_{Ts} + EI_\omega G''I_{Ts}))^2) \end{aligned}$
$\eta_1(x) =$
$\begin{aligned} & - (((GI_{Ts})^3 (-GI_T + \omega^2 \rho I_\omega) + 2EI_\omega GI_T (GI_{Ts})^2 + (GI_{Ts})^2 (\omega^2 \rho I_\omega GI_T + EI_\omega GI_T + EI_\omega (\omega^2 \rho I_p + G''I_T))) \\ & - GI_{Ts} ((GI_T E'I_\omega + 2EI_\omega GI_T) GI_T + EI_\omega GI_T G''I_{Ts})) ((GI_{Ts})^2 (3GI_{Ts} - \omega^2 \rho' I_\omega) - GI_{Ts} (EI_\omega GI_{Ts} + 3EI_\omega G''I_{Ts})) \\ & + GI_{Ts} (GI_{Ts} (-2\omega^2 \rho I_\omega + E''I_\omega) + 2EI_\omega G''I_{Ts} + EI_\omega G'''I_{Ts})) - (((GI_{Ts})^3 - \omega^2 \rho I_\omega (GI_{Ts})^2 - 2EI_\omega (GI_{Ts})^2 \\ & + GI_{Ts} (EI_\omega GI_{Ts} + EI_\omega G''I_{Ts})) ((GI_{Ts})^3 (-GI_T + \omega^2 \rho' I_\omega) + GI_T GI_{Ts} (EI_\omega GI_{Ts} + 3EI_\omega G''I_{Ts})) \\ & + (GI_{Ts})^2 (2\omega^2 \rho I_p E'I_\omega + \omega^2 \rho I_\omega (GI_T + 3GI_{Ts}) + GI_T (-3GI_{Ts} + \omega^2 \rho' I_\omega) + GI_T E''I_\omega + 2EI_\omega G''I_T \\ & + EI_\omega (2\omega^2 \rho' I_\omega + G'''I_T)) - GI_{Ts} (GI_T (EI_\omega GI_{Ts} + 3EI_\omega G''I_{Ts}) + GI_T (GI_{Ts} (-2\omega^2 \rho' I_\omega + E''I_\omega) \\ & + 2EI_\omega G''I_{Ts} + EI_\omega G'''I_{Ts}))) / (((GI_{Ts})^3 - \omega^2 \rho I_\omega (GI_{Ts})^2 - 2EI_\omega (GI_{Ts})^2 + GI_{Ts} (EI_\omega GI_{Ts} + EI_\omega G''I_{Ts}))^2) \end{aligned}$

$\eta_2(x) =$
$\begin{aligned} & -((GI_{Ts}(-((GI_{Ts})^3 - \omega^2(GI_{Ts})^2 \rho I_{\omega} - 2EI_{\omega}(G'I_{Ts})^2 + GI_{Ts}(E'I_{\omega}G'I_{Ts} + EI_{\omega}G''I_{Ts}))) (GI_{Ts}(E'I_{\omega}(4G'I_T + 3G'I_{Ts}) \\ & + GI_{Ts}(\omega^2 \rho I_{\omega} + E''I_{\omega})) + EI_{\omega}(\omega^2 \rho I_{\rho} + 3G''I_T)) - GI_T((GI_{Ts})^2 + E'I_{\omega}G'I_{Ts} - GI_{Ts}(\omega^2 \rho I_{\omega} + E''I_{\omega}) + 3EI_{\omega}G''I_{Ts})) \\ & + (GI_{Ts}((GI_T + GI_{Ts})E'I_{\omega} + 2EI_{\omega}G'I_T) - 2EI_{\omega}GI_TG'I_{Ts})(GI_{Ts}^2(3G'I_{Ts} - \omega^2 \rho' I_{\omega}) - G'I_{Ts}(E'I_{\omega}G'I_{Ts} + 3EI_{\omega}G''I_{Ts}) \\ & + GI_{Ts}(G'I_{Ts}(-2\omega^2 \rho I_{\omega} + E''I_{\omega})) + 2E'I_{\omega}G''I_{Ts} + EI_{\omega}G'''I_{Ts})))) / ((GI_{Ts})^3 - \omega^2(GI_{Ts})^2 \rho I_{\omega} - 2EI_{\omega}(G'I_{Ts})^2 \\ & + GI_{Ts}(E'I_{\omega}G'I_{Ts} + EI_{\omega}G''I_{Ts}))^2 \end{aligned}$

$\eta_3(x) =$
$\begin{aligned} & -((GI_{Ts})^2(-2(GI_T + GI_{Ts})E'I_{\omega} + 3EI_{\omega}(G'I_T + G'I_{Ts}))((GI_{Ts})^3 - \omega^2 \rho I_{\omega}(GI_{Ts})^2 - 2EI_{\omega}(G'I_{Ts})^2 \\ & + GI_{Ts}(E'I_{\omega}G'I_{Ts} + EI_{\omega}G''I_{Ts})) + EI_{\omega}(GI_T + GI_{Ts})((GI_{Ts})^2(3G'I_{Ts} - \omega^2 \rho' I_{\omega}) \\ & - G'I_{Ts}(E'I_{\omega}G'I_{Ts} + 3EI_{\omega}G''I_{Ts}) + GI_{Ts}(G'I_{Ts}(-2\omega^2 \rho I_{\omega} + E''I_{\omega})) + 2E'I_{\omega}G''I_{Ts} + EI_{\omega}G'''I_{Ts}))) \\ & / ((GI_{Ts})^3 - \omega^2 \rho I_{\omega}(GI_{Ts})^2 - 2EI_{\omega}(G'I_{Ts})^2 + GI_{Ts}(E'I_{\omega}G'I_{Ts} + EI_{\omega}G''I_{Ts}))^2 \end{aligned}$

$\eta_4(x) =$
$\frac{EI_{\omega}(GI_{Ts})^2(GI_T + GI_{Ts})}{(GI_{Ts})^3 - \omega^2 \rho I_{\omega}(GI_{Ts})^2 - 2EI_{\omega}(G'I_{Ts})^2 + GI_{Ts}(E'I_{\omega}G'I_{Ts} + EI_{\omega}G''I_{Ts})}$

The load polynomial, for several load conditions, on the right-hand side of (19), reads as:

$\eta_L(x) = \sum_{s=0}^{\max s} \eta_{L,s} x^s =$	
$m_T \neq 0$	$\begin{aligned} & m_T(-1 - ((GI_{Ts})^3 - \omega^2(GI_{Ts})^2 \rho I_{\omega} - 2EI_{\omega}(G'I_{Ts})^2 + GI_{Ts}(E'I_{\omega}G'I_{Ts} + EI_{\omega}G''I_{Ts})) \\ & ((GI_{Ts})^2 E''I_{\omega} - 2EI_{\omega}((G'I_{Ts})^2 + GI_{Ts}G''I_{Ts})) + GI_{Ts}(GI_{Ts}E'I_{\omega} - 2EI_{\omega}G'I_{Ts}) \\ & (GI_{Ts}^2(3G'I_{Ts} - \omega^2 \rho' I_{\omega}) - G'I_{Ts}(E'I_{\omega}G'I_{Ts} + 3EI_{\omega}G''I_{Ts}) + GI_{Ts}(G'I_{Ts}(-2\omega^2 \rho I_{\omega} + E''I_{\omega}) \\ & + 2E'I_{\omega}G''I_{Ts} + EI_{\omega}G'''I_{Ts})))) / ((GI_{Ts})^3 - \omega^2 \rho I_{\omega}(GI_{Ts})^2 - 2EI_{\omega}(G'I_{Ts})^2 \\ & + GI_{Ts}(E'I_{\omega}G'I_{Ts} + EI_{\omega}G''I_{Ts}))^2 \end{aligned}$
$m'_T \neq 0$	$\begin{aligned} & m'_T(((GI_{Ts})^2(2(GI_{Ts})^3 E'I_{\omega} + (GI_{Ts})^2(-3EI_{\omega}G'I_{Ts} + \omega^2(-2\rho I_{\omega}E'I_{\omega} + EI_{\omega}\rho' I_{\omega})) + 3EI_{\omega}G'I_{Ts} \\ & (-E'I_{\omega}G'I_{Ts} + EI_{\omega}G''I_{Ts}) + GI_{Ts}(G'I_{Ts}(2(E'I_{\omega})^2 + EI_{\omega}(2\omega^2 \rho I_{\omega} - E''I_{\omega})) - (EI_{\omega})^2 G'''I_{Ts}))) \\ & / ((GI_{Ts})^3 - \omega^2 \rho I_{\omega}(GI_{Ts})^2 - 2EI_{\omega}(G'I_{Ts})^2 + GI_{Ts}(E'I_{\omega}G'I_{Ts} + EI_{\omega}G''I_{Ts}))^2 \end{aligned}$
$m''_T \neq 0$	$m''_T((EI_{\omega}(GI_{Ts})^2) / ((GI_{Ts})^3 - \omega^2 \rho I_{\omega}(GI_{Ts})^2 - 2EI_{\omega}(G'I_{Ts})^2 + GI_{Ts}(E'I_{\omega}G'I_{Ts} + EI_{\omega}G''I_{Ts})))$
$m_{\omega} \neq 0$	$\begin{aligned} & m_{\omega}(((GI_{Ts})^2(-6EI_{\omega}(G'I_{Ts})^3 + \omega^2 \rho' I_{\omega}(GI_{Ts})^3 + 2GI_{Ts}G'I_{Ts}(2E'I_{\omega}G'I_{Ts} + 3EI_{\omega}G''I_{Ts}) \\ & - (GI_{Ts})^2(G'I_{Ts}(\omega^2 \rho I_{\omega} + E''I_{\omega}) + 2E'I_{\omega}G''I_{Ts} + EI_{\omega}G'''I_{Ts})))) \\ & / ((GI_{Ts})^3 - \omega^2 \rho I_{\omega}(GI_{Ts})^2 - 2EI_{\omega}(G'I_{Ts})^2 + GI_{Ts}(E'I_{\omega}G'I_{Ts} + EI_{\omega}G''I_{Ts}))^2 \end{aligned}$
$m'_{\omega} \neq 0$	$m'_{\omega}(GI_{Ts})^3 / ((GI_{Ts})^3 - \omega^2 \rho I_{\omega}(GI_{Ts})^2 - 2EI_{\omega}(G'I_{Ts})^2 + GI_{Ts}(E'I_{\omega}G'I_{Ts} + EI_{\omega}G''I_{Ts}))$

A2. Coefficients of the Transformation matrix T .

Firstly, the transformation matrix \mathbf{T} is derived. It transforms the vector \mathbf{Z}_x to the vector $\boldsymbol{\psi}$, i.e $\boldsymbol{\psi} = \mathbf{T} \cdot \mathbf{Z}_x$:

$$\begin{bmatrix} \boldsymbol{\psi} \\ \psi(x) \\ \psi'(x) \\ \psi''(x) \\ \psi'''(x) \\ 1 \end{bmatrix} = \begin{bmatrix} T_{1,1}(x) & T_{1,2}(x) & T_{1,3}(x) & T_{1,4}(x) & T_{1,5}(x) \\ T_{2,1}(x) & T_{2,2}(x) & T_{2,3}(x) & T_{2,4}(x) & T_{2,5}(x) \\ T_{3,1}(x) & T_{3,2}(x) & T_{3,3}(x) & T_{3,4}(x) & T_{3,5}(x) \\ T_{4,1}(x) & T_{4,2}(x) & T_{4,3}(x) & T_{4,4}(x) & T_{4,5}(x) \\ 0 & 0 & 0 & 0 & 1 \end{bmatrix} \begin{bmatrix} \mathbf{Z}_x \\ \psi(x) \\ \psi'_M(x) \\ M_\omega(x) \\ M_T(x) \\ 1 \end{bmatrix}. \quad (32)$$

The first line of the transformation matrix \mathbf{T} reads as

$$T_{1,1} = 1, \quad T_{1,2} = 0, \quad T_{1,3} = 0, \quad T_{1,4} = 0, \quad T_{1,5} = 0. \quad (33)$$

Substitution of (14) into (12) gives

$$\psi'(x) = \psi'_M(x) + \psi'_S(x) = \psi'_M(x) + \frac{M_{Ts}(x)}{G(x)I_{Ts}}. \quad (34)$$

Inserting $M_{Tp}(x)$, obtained from (13), into (10) yields

$$M_{Ts}(x) = M_T(x) - G(x)I_T\psi'(x). \quad (35)$$

Substitution of (35) into (34) gives

$$\psi'(x) = \left(\frac{G(x)I_{Ts}}{G(x)I_{Ts} + G(x)I_T} \right) \psi'_M(x) + \left(\frac{1}{G(x)I_{Ts} + G(x)I_T} \right) M_T(x). \quad (36)$$

The second line of the transformation matrix \mathbf{T} reads as

$$T_{2,1} = 0, \quad T_{2,2} = \frac{GI_{Ts}}{GI_{Ts} + GI_T}, \quad T_{2,3} = 0, \quad T_{2,4} = \frac{1}{GI_{Ts} + GI_T}, \quad T_{2,5} = 0. \quad (37)$$

Inserting $\psi''_M(x)$, obtained from (11), and $M'_T(x)$, obtained from (8), into the expression for $\psi''(x)$, obtained from derivation of (36) with respect to x , yields the third line of the transformation matrix:

$$\begin{aligned} T_{3,1} &= -\frac{\omega^2 \rho I_p}{GI_{Ts} + GI_T}, & T_{3,2} &= \frac{-GI_{Ts}GI_T + GI_TGI_{Ts}}{(GI_{Ts} + GI_T)^2}, \\ T_{3,3} &= -\frac{GI_{Ts}}{EI_\omega(GI_{Ts} + GI_T)}, & T_{3,4} &= -\frac{GI_T + GI_{Ts}}{(GI_{Ts} + GI_T)^2}, & T_{3,5} &= -\frac{m_T}{GI_{Ts} + GI_T}. \end{aligned} \quad (38)$$

The fourth line of the transformation matrix is obtained from the second derivative of (36) with respect to x . The resulting expression for $\psi'''(x)$ contains $\psi'(x)$, $\psi''_M(x)$, $M'_\omega(x)$, and $M'_T(x)$. $\psi''_M(x)$ is given in (11) and $M'_T(x)$ in (8). $M'_\omega(x)$ is obtained

from (9) after inserting $\psi'_M(x)$ from (34) and $M_{T_S}(x)$ from (35) into (9). In this way, the fourth line of the transformation matrix is obtained as follows:

$$\begin{aligned}
T_{41} &= \frac{\omega^2(2\rho I_p(G'I_{T_S} + G'I_T) - (GI_{T_S} + GI_T)\rho'I_p)}{(GI_{T_S} + GI_T)^2}, \\
T_{42} &= \frac{1}{(GI_{T_S} + GI_T)^3} \left(\frac{GI_{T_S}(GI_T + GI_{T_S})(GI_T GI_{T_S} - \omega^2(GI_T + GI_{T_S})\rho I_\omega)}{EI_\omega} \right. \\
&\quad - GI_{T_S}(-2G'I_T(G'I_{T_S} + G'I_T) + GI_{T_S}(\omega^2\rho I_p + G''I_T)) \\
&\quad \left. - GI_T(2G'I_{T_S}(G'I_{T_S} + G'I_T) + GI_{T_S}(\omega^2\rho I_\omega + G''I_T - G''I_{T_S})) + GI_T^2 G''I_{T_S} \right), \\
T_{43} &= \frac{GI_{T_S}((GI_{T_S} + GI_T)EI_\omega + 2EI_\omega G'I_T) - 2EI_\omega GI_T G'I_{T_S}}{EI_\omega^2(GI_{T_S} + GI_T)^2}, \\
T_{44} &= -\frac{(GI_{T_S})^3 - 2EI_\omega(G'I_T + G'I_{T_S})^2 + EI_\omega GI_{T_S}(\omega^2\rho I_p + G''I_T + G''I_{T_S})}{EI_\omega(GI_{T_S} + GI_T)^3} + \\
&\quad \frac{GI_T((GI_{T_S})^2 + EI_\omega(\omega^2\rho I_p + G''I_T + G''I_{T_S}))}{EI_\omega(GI_{T_S} + GI_T)^3}, \\
T_{45} &= -\frac{GI_{T_S}m_\omega}{EI_\omega(GI_{T_S} + GI_T)} + \frac{2m_T(G'I_T + G'I_{T_S})}{(GI_{T_S} + GI_T)^2} - \frac{m'_T}{GI_{T_S} + GI_T}. \tag{39}
\end{aligned}$$

Secondly, the load vector and the matrix \mathbf{b} in (22) are established. The matrix \mathbf{A} , which is needed for (23), follows from

$$\mathbf{A} = \mathbf{T}^{-1} \mathbf{b} \mathbf{T}|_{x=0} = \mathbf{T}^{-1} \mathbf{b} \mathbf{T}_i. \tag{40}$$

A3. Coefficients of the matrix \mathbf{B} in (24).

$$\begin{aligned}
B_{1,1} &= -\frac{A_{1,3}A_{2,1} - A_{1,2}A_{2,3}}{-A_{1,4}A_{2,3} + A_{1,3}A_{2,4}}, B_{2,1} = \frac{-A_{1,4}A_{2,2} - A_{1,2}A_{2,4}}{-A_{1,4}A_{2,3} + A_{1,3}A_{2,4}}, \\
B_{3,1} &= A_{4,1} - \frac{A_{1,1}A_{4,3}}{A_{1,3}} + \frac{A_{1,4}A_{2,1}A_{4,3}}{-A_{1,4}A_{2,3} + A_{1,3}A_{2,4}} - \frac{A_{1,1}A_{1,4}A_{2,3}A_{4,3}}{A_{1,3}(-A_{1,4}A_{2,3} + A_{1,3}A_{2,4})} - \frac{A_{1,3}A_{2,1}A_{4,4}}{-A_{1,4}A_{2,3} + A_{1,3}A_{2,4}} \\
&\quad + \frac{A_{1,1}A_{2,3}A_{4,4}}{-A_{1,4}A_{2,3} + A_{1,3}A_{2,4}}, \\
B_{4,1} &= \frac{A_{1,4}A_{2,3}A_{3,1} - A_{1,3}A_{2,4}A_{3,1} - A_{1,4}A_{2,1}A_{3,3} + A_{1,1}A_{2,4}A_{3,3} + A_{1,3}A_{2,1}A_{3,4} - A_{1,1}A_{2,3}A_{3,4}}{-A_{1,4}A_{2,3} + A_{1,3}A_{2,4}},
\end{aligned}$$

$$\begin{aligned}
B_{1,2} &= -\frac{A_{1,3}A_{2,1} - A_{1,2}A_{2,3}}{-A_{1,4}A_{2,3} + A_{1,3}A_{2,4}}, B_{2,2} = \frac{-A_{1,4}A_{2,2} - A_{1,2}A_{2,4}}{-A_{1,4}A_{2,3} + A_{1,3}A_{2,4}}, \\
B_{3,2} &= A_{4,2} - \frac{A_{1,2}A_{4,3}}{A_{1,3}} + \frac{A_{1,4}A_{2,2}A_{4,3}}{-A_{1,4}A_{2,3} + A_{1,3}A_{2,4}} - \frac{A_{1,2}A_{1,4}A_{2,3}A_{4,3}}{A_{1,3}(-A_{1,4}A_{2,3} + A_{1,3}A_{2,4})}, \\
B_{4,2} &= \frac{A_{1,4}A_{2,3}A_{3,2} - A_{1,3}A_{2,4}A_{3,2} - A_{1,4}A_{2,2}A_{3,3} + A_{1,2}A_{2,4}A_{3,3} + A_{1,3}A_{2,2}A_{3,4} - A_{1,2}A_{2,3}A_{3,4}}{-A_{1,4}A_{2,3} + A_{1,3}A_{2,4}}, \\
B_{1,3} &= -\frac{A_{2,3}}{-A_{1,4}A_{2,3} + A_{1,3}A_{2,4}}, B_{2,3} = \frac{A_{2,4}}{-A_{1,4}A_{2,3} + A_{1,3}A_{2,4}}, \\
B_{3,3} &= \frac{A_{4,3}}{A_{1,3}} - \frac{A_{2,3}A_{4,4}}{-A_{1,4}A_{2,3} + A_{1,3}A_{2,4}} + \frac{A_{1,4}A_{2,3}A_{4,3}}{A_{1,3}(-A_{1,4}A_{2,3} + A_{1,3}A_{2,4})}, \\
B_{4,3} &= \frac{-A_{2,4}A_{3,3} + A_{2,3}A_{3,4}}{-A_{1,4}A_{2,3} + A_{1,3}A_{2,4}}, B_{1,4} = \frac{A_{1,3}}{A_{1,4}A_{2,3} - A_{1,3}A_{2,4}}, B_{2,4} = -\frac{A_{1,4}}{A_{1,4}A_{2,3} - A_{1,3}A_{2,4}}, \\
B_{3,4} &= \frac{A_{1,4}A_{4,3} - A_{1,3}A_{4,4}}{-A_{1,4}A_{2,3} + A_{1,3}A_{2,4}}, B_{4,4} = -\frac{A_{1,4}A_{3,3}}{-A_{1,4}A_{2,3} + A_{1,3}A_{2,4}} + \frac{A_{1,3}A_{3,4}}{-A_{1,4}A_{2,3} + A_{1,3}A_{2,4}}, \\
F_1 &= \frac{A_{1,5}A_{2,3} - A_{1,3}A_{2,5}}{-A_{1,4}A_{2,3} + A_{1,3}A_{2,4}}, F_2 = \frac{A_{1,5}A_{2,4} - A_{1,4}A_{2,5}}{A_{1,4}A_{2,3} - A_{1,3}A_{2,4}}, \\
F_3 &= \frac{A_{1,5}A_{2,4}A_{4,3} - A_{1,4}A_{2,5}A_{4,3} - A_{1,5}A_{2,3}A_{4,4} + A_{1,3}A_{2,5}A_{4,4}}{A_{1,4}A_{2,3} - A_{1,3}A_{2,4}} + A_{4,5}, \\
F_4 &= \frac{A_{1,5}A_{2,4}A_{4,3} - A_{1,4}A_{2,5}A_{3,3} - A_{1,5}A_{2,3}A_{3,4} + A_{1,3}A_{2,5}A_{3,4}}{-A_{1,4}A_{2,3} - A_{1,3}A_{2,4}} + A_{3,5}.
\end{aligned}$$

Acknowledgements

The authors gratefully acknowledge financial support by the Slovak Grant Agency: VEGA No. 1/0102/18 and open access funding provided by Austrian Science Fund (FWF): M 2009-N32.

References

- [1] Aminbaghai M, Murin J, Hrabovsky J, Mang HA. Torsional warping eigenmodes including the effect of the secondary torsion moment on the deformations. Eng Struct 2016; 106: 299 – 316.
- [2] Dikaros IC, Sapountzakis EJ, Argyridi AK. Generalized warping effect in the dynamic analysis of beams of arbitrary cross Chapter. J Sound Vib 2016; 369: 119 – 146.

- [3] ANSYS Swanson Analysis System, Inc., 201 Johnson Road, Houston, PA 15342/1300, USA.
- [4] ADINA R & D, Inc. Theory and Modelling Guide. Volume I: ADINA. 2013.
- [5] ABAQUS/CAE, Version 6.10-1, Dassault Systems Simulia Corp. Providence, RI, USA.
- [6] Przemieniecki JS. Theory of matrix structural analysis. McGraw-Hill, NY, 1968.
- [7] Bathe KJ, Chaudhary A. On the displacement formulation of torsion of shafts with rectangular cross-sections, *Int Numer Methods Eng* 1982; 18: 1565 – 1568.
- [8] Sapountzakis EJ, Tsipiras VJ, Argyridi AK. Torsional vibration analysis of bars including secondary torsional shear deformation effect by the boundary element method. *Journal of Sound and Vibration* 2015; 355: 208 – 231.
- [9] Sapountzakis EJ, Mokos VG. Dynamic analysis of 3-D beam elements including warping and shear deformation effects. *Solids and Structures* 2006; 43: 6707 – 6726.
- [10] Sapountzakis EJ, Tsipiras VJ. Nonlinear non-uniform torsional vibration. *Non-linear Mechanics* 2010; 329: 1853 – 1874.
- [11] Sapountzakis EJ, Dikaros IC. Non-linear flexural – torsional dynamic analysis of beams of arbitrary cross Chapter by BEM. *Non-linear Mechanics* 2011; 46: 782 – 794.
- [12] Sina SA, Haddadpour H, Navazi HM. Nonlinear free vibration of thin walled beams in torsion. *Acta Mechanica* 2012; 233: 2135 – 2151.
- [13] Lee SJ, Park SB. Vibrations of Timoshenko beams with isogeometric approach. *Applied Mathematical Modelling* 2013; 37: 9174 – 9190.
- [14] Stoykov S, Ribeiro P. Non-linear vibrations of beams with non-symmetrical cross Chapters. *Non-linear Mechanics* 2013; 55: 153 – 169.
- [15] Sina SA, Haddadpour H. Axial – torsional vibrations of rotated pre twisted thin walled composite beams. *Mechanical Sciences* 2014; 80: 93 – 101.
- [16] Ferradi KF, Cespedes X. A new beam element with transversal and warping eigenmodes. *Computers and Structures* 2014; 131: 12 – 33.
- [17] Yoon K, Kim DN. Geometrically nonlinear analysis of functionally graded 3D beams considering warping effects. *Composite Structures* 2015; 132: 1231–1247.
- [18] Murin J, Aminbaghai M, Kutis V, Kralovic V, Goga V, Mang HA. A new 3D Timoshenko finite beam element including non-uniform torsion of open and closed cross Chapters. *Eng Struct* 2014; 59: 153 – 160.
- [19] Murin J, Goga V, Aminbaghai M, Hrabovsky J, Sedlar T, Mang HA. Measurement and modelling of torsional warping free vibrations of beams with rectangular hollow cross-sections. *Eng Struct* 2017; 136: 68 – 76.
- [20] Rubin H. Lösung linearer Differentialgleichungen beliebiger Ordnung mit Polynomkoeffizienten und Anwendung auf ein baustatisches Problem [in German: *Solution of linear differential equations of arbitrary order with*

- polynomial coefficients and application to a problem of structural analysis*].
Zeitschrift für Angewandte Mathematik und Mechanik 1996; 76(2): 105–117.
- [21] Aminbaghai M, Dorn M, Pichler B, Eberhardsteiner J. A matrix-vector operation-based numerical solution method for linear m-th order ordinary differential equations: application to engineering problems. *Advances in Applied Mathematics and Mechanics* 2013; 3: 269 – 308.
- [22] Wolfram Mathematica 9.0.1.0, Wolfram Research 2013.
- [23] Hrabovsky J, Murin J, Aminbaghai M, Kutis V, Paulech J. Numerical solution of differential equations with non-constant coefficients. *ECCOMAS Congress 2016. Volume I - IV: Proceedings of the VII European congress on computational methods in applied sciences and engineering. Crete, Greece, 5 – 10 June 2016*, S. 4878-4887. ISBN 978-618-82844-0-1
- [24] Tsipsis IN, Sapountzakis EJ. Generalized warping and distortional analysis of curved beams with isogeometric methods. *Comp and Struct* 2017; 191: 33 – 50.
- [25] Rubin H. Wölbkrafttorsion von Durchlaufträgern mit konstantem Querschnitt unter Berücksichtigung sekundärer Schubverformung [in German; *Torsional warping theory including the secondary torsion-moment deformation-effect for beams with constant cross-section*]. *Stahlbau* 2005; 74: 826 – 842.
- [26] Aminbaghai M, Murin J, Balduzzi G, Hrabovsky J, Hochreiner G, Mang HA. Second-order torsional warping theory considering the secondary torsion-moment deformation-effect. *Eng Struct* 2017; 147: 724 – 739.
- [27] Murin J, Aminbaghai M, Hrabovsky J, Gogola R, Kugler S. Beam finite element for modal analysis of FGM structures. *Eng Struct* 2016; 121: 1 – 18.